Serb. Astron. J. № 177 (2008), 53 - 59
DOI: 10.2298/SAJ0877053P

UDC 524.37-355.3 : 524.722.3
Original scientific paper

OPTICAL SPECTRA OF RADIO PLANETARY NEBULAE IN THE LARGE MAGELLANIC CLOUD

J. L. Payne[1], M. D. Filipović[2], W. C. Millar[1], E. J. Crawford[2], A. Y. De Horta[2], F. H. Stootman[2] and D. Urošević[3]

[1] *Centre for Astronomy, James Cook University Townsville QLD, 4811, Australia*

E–mail: *snova4@msn.com*

[2] *University of Western Sydney, Locked Bag 1797 Penrith South, DC, NSW 1797, Australia*

[3] *Department of Astronomy, Faculty of Mathematics, University of Belgrade Studentski trg 16, 11000 Belgrade, Serbia*

(Received: July 9, 2008; Accepted: August 19, 2008)

SUMMARY: We present 11 spectra from 12 candidate radio sources co-identified with known planetary nebulae (PNe) in the Large Magellanic Cloud (LMC). Originally found in Australia Telescope Compact Array (ATCA) LMC surveys at 1.4, 4.8 and 8.64 GHz and confirmed by new high resolution ATCA images at 6 and 3 cm ($4''/2''$), these complement data recently presented for candidate radio PNe in the Small Magellanic Cloud (SMC). Their spectra were obtained using the Radcliffe 1.9-meter telescope in Sutherland (South Africa). All of the optical PNe and radio candidates are within $2''$ and may represent a population of selected radio bright sample only. Nebular ionized masses of these objects are estimated to be as high as 1.8 $M_{\odot}$, supporting the idea that massive PNe progenitor central stars lose much of their mass in the asymptotic giant branch (AGB) phase or prior. We also identify a sub-population (33%) of radio PNe candidates with prominent ionized iron emission lines.

Key words. planetary nebulae: individual: SMP L8, SMP L25, SMP L33, SMP L39, SMP L47, SMP L62, SMP L74, SMP L75, SMP L83, SMP L84, SMP L89

1. INTRODUCTION

Planetary nebulae (PNe) are one of the most important processes giving rise to and sustaining the chemical evolution of galaxies, contributing about half of the overall enrichment of the interstellar medium. They are the product of lower-mass stars where the central-star and nebular masses are only about 0.6 and 0.3 $M_{\odot}$, respectively. However, detection of white dwarfs in open clusters suggests the main-sequence mass of PNe progenitors can be as high as 8 $M_{\odot}$ (Kwok 1994). Because they contain the products of the nuclear reactions occurring in the later stages of stellar evolution, they have high levels of helium, nitrogen, oxygen and carbon. Their expansion into the interstellar environment carries these products into the galactic disk. It is very likely that PNe are a greater contributer to the galactic N/O abundance than super-

novae remnants. The over-abundance of these elements in typical PNe allows us to support the confirmation of a candidate PN with optical spectra by measuring abundance ratios of these elements. Optical spectral requirements for the confirmation of PNe have been summarised very nicely by Reid and Parker (2006). Classically, PNe can be identified by a [O III]5007Å:[O III]4959Å:Hβ intensity ratio near 9:3:1. This can be relaxed when the intensity of [N II]6583Å is greater than Hα. In that case, a strong [O III] line has been often detected along with the high excitation He II4686Å line hardly seen in H II regions. Generally, the [O II]3727Å doublet is seen in PNe, as well as [Ne III]3869Å, [Ar III]7135Å and He I6678Å lines. [S II]6717, 6731Å are usually present but not significant when compared to Hα.

The study of extra-Galactic PNe is crucial to the understanding of PNe in general. Observations of Galactic PNe are hampered by the uncertain distances. While the population of nearby Galactic PNe is not small, we can drastically expand our understanding of Galactic PNe by studying PNe in other, nearby galaxies, such as the Magellanic Clouds (MCs).

In this paper we present optical spectra of 11 PNe that co-identify with radio PNe candidates recently found in the Large Magellanic Cloud (LMC). Spectra of four (4) PNe with radio counterparts were recently presented for the Small Magellanic Cloud (SMC) in Payne et al. (2008). Section 2 details our spectral observations and reduction methods used to calibrate the data analysed in Section 3. The paper concludes with some final comments and a brief summary as presented in Section 4.

2. OBSERVATIONS

The first radio PNe candidate of this series was reported in Payne et al. (2004). Since, ∼17 have been found within a few arcseconds of known optical PNe in the direction of the Magellanic Clouds (Filipović et al., in prep.). This includes at least 12 LMC sources from Australia Telescope Compact Array (ATCA) observations, complemented with short-spacings using Parkes data and reduced using the MIRIAD software suite to create mosaic images at 1.4 GHz (Hughes et al. 2007), and 4.8, 8.64 GHz (Dickel et al. 2005). Recent followup ATCA observations at 4.8 and 8.64 GHz give much higher resolutions ($4''/2''$) and appear to confirm that most are bright radio counterparts within $2''$ of known optical PNe. The number and flux densities of these candidate radio PNe are unexpected given the distance of the LMC of ∼ 50 kpc (Alves 2004). This may well modify our current understanding of PNe, including their progenitor mass and evolution.

Here, we present optical spectra for the radio candidates shown in Fig. 1 and listed in Table 1. For each, we give its radio name, position (adopted from the highest available frequency), difference of radio and optical positions, radio spectral index, 4.8 GHz flux density, estimated ionized mass and optical counterpart PNe names. These known optical PNe have been found in surveys including Sanduleak et al. (1978) and Read and Parker (2006). From Table 1, we also note that our spectral indices support the general belief that PNe are dominant thermal radio emitters.

Spectral observations were conducted in January 2008, using the 1.9-meter telescope and Cassegrain spectrograph at the South African Astronomical Observatory (SAAO) in Sutherland. We used grating number 7 (300 lpmm) to obtain spectra between 3500 and 6200 Å having a resolution of 5 Å. For these, the slit size was $1.5'' \times 1.5'$ with a spatial resolution of $0.74''$ pixel^{-1}. Exposure times were limited to 800 s with a positional accuracy of $< 1''$.

Data reduction included bias subtraction and flat-field correction using the IRAF software package. Extraction (task 'extractor'), including background sky subtraction, of data allowed the creation of one-dimensional spectra, with wavelength calibrated using standard lines from a CuAr arc. Flux calibration was applied using the spectrometric standard star EG 21. Observing conditions were fair with seeing limited to $>1''$ but varied throughout the night.

3. SPECTRAL ANALYSIS

If one assumes that these PNe have a relatively symmetric uniform density, it may be possible to crudely estimate their ionized mass ($M_{\rm i}$):

$$M_{\rm i} = 282(D_{\rm kpc})^2 F_5 (n_{\rm e})^{-1} M_{\odot}, \qquad (1)$$

where $D_{\rm kpc}$ is distance (kpc), F_5 is radio flux density at ∼ 5 GHz (Jy) and $n_{\rm e}$ represents assumed electron density (10^3 cm^{-3}) (Kwok 2000). Table 1 lists an ionized mass estimate for each PN based on the given flux densities at 4.8 GHz. These values, as high as 1.8 $M_{\odot}$, imply our selected radio bright objects may have higher nebular ionized masses than previously expected.

We used IRAF's task SPLOT to view and analyze our spectra. Only fluxes from spectral lines visually distinct from the baseline rms (∼ 10^{-15} ergs cm^{-2} s^{-1} Å^{-1}) were selected for inclusion in Table 2. For each PNe, Table 2 lists the relative flux densities (using EG21) and 90% confidence intervals of common lines within our spectral range. These lines include the [O II]3727Å doublet, [Ne III]3869Å, H$\beta\lambda$4861Å and [O III]4363, 4959, 5007Å. All values are shown at their rest wavelengths.

Table 1. Radio PN candidates in the LMC with available spectra from our study. ΔP represents the distance between radio and optical positions. SMP refers to Sanduleak et al. (1978). Spectral index (α) is defined here as $S_\nu \propto \nu^\alpha$, where S_ν is the flux density at frequency ν. Ionized mass (M_i) assumes an electron density (n_e) of 10^3 cm^{-3}.

No.	ATCA Radio Source Name	R.A. (J2000.0)	Dec. (J2000.0)	ΔP (arcsec)	$\alpha \pm \Delta\alpha$	$S_{4.8\mathrm{GHz}}$ (mJy)	M_i ($M_\odot$)	Optical PN Name
1	LMC J045013-693352	04 50 13.28	–69 33 52.7	1″	—	—	—	SMP L8
2	LMC J050624-690320	05 06 24.22	–69 03 20.1	1″	0.2±0.3	2.1	1.5	SMP L25
3	LMC J051009-682955	05 10 09.38	–68 29 55.1	1″	—	—	—	SMP L33
4	LMC J051142-683459	05 11 42.11	–68 34 59.1	1″	—	—	—	SMP L39
5	LMC J051954-693104	05 19 54.51	–69 31 04.5	2″	0.0±0.2	2.1	1.5	SMP L47
6	LMC J052455-713255	05 24 55.31	–71 32 55.0	1″	–0.2±0.2	2.1	1.5	SMP L62
7	LMC J053329-715227	05 33 29.09	–71 52 27.2	2″	–0.7±0.3	1.1	0.8	SMP L74
8	LMC J053346-683643	05 33 46.90	–68 36 43.0	2″	—	—	—	SMP L75
9	LMC J053620-671807	05 36 20.69	–67 18 07.9	< 1″	–0.3±0.2	0.9	0.6	SMP L83
10	LMC J053653-715339	05 36 53.46	–71 53 39.3	2″	—	—	—	SMP L84
11	LMC J054237-700930	05 42 37.17	–70 09 30.4	2″	–0.1±0.2	2.6	1.8	SMP L89

Table 2. Spectral analysis of known optical PNe co-incident with radio sources. Flux densities are given in units of 10^{-14} ergs cm^{-2} s^{-1} and include 90 % confidence intervals. Electron temperature (T_e) assumes an electron density (n_e) of 10^3 cm^{-3}. There is no correction for extinction.

Name	[O II] 3727Å	[Ne III] 3869Å	[O III] 4363Å	Hβ 4861Å	[O III] 4959Å	[O III] 5007Å	Hγ/Hβ	E(B–V)	T_e (K)
SMP L8	—	51.0±1.0	18.4±0.6	35.4±0.9	70.8±0.9	207.3±1.0	0.7	–0.9	49760
SMP L25	118.5±1.1	185.5±1.0	26.1±1.1	144.4±1.0	380.5±1.0	1110.0±0.9	0.7	–0.9	16430
SMP L33	86.9±1.1	33.9±0.9	2.8±0.8	16.1±1.0	68.0±1.0	198.1±1.0	0.8	–1.2	13039
SMP L39	10.7±1.0	—	—	0.9±0.9	3.7±0.9	11.1±0.9	—	—	—
SMP L47	1112.0±1.2	676.0±1.1	36.5±1.0	124.1±0.9	395.3±1.0	1183.0±1.0	0.7	–0.9	19056
SMP L62	6.1±1.2	11.3±1.0	3.9±0.9	21.3±1.0	77.8±0.8	236.7±1.0	0.4	0.6	14039
SMP L74	14.5±1.2	14.0±0.9	2.6±1.1	13.8±0.9	57.1±0.9	172.5±1.0	0.5	–0.2	13409
SMP L75	—	12.3±1.0	1.8±1.2	18.7±0.9	57.5±0.9	173.1±1.0	1.0	–1.6	11696
SMP L83	—	9.0±1.0	3.3±1.5	10.1±1.1	28.7±0.9	85.5±1.0	0.5	–0.3	21941
SMP L84	—	—	1.8±1.1	11.5±1.0	25.8±0.9	78.8±0.9	—	—	16473
SMP L89	1203.0±1.1	1279.0±1.1	116.1±1.4	181.2±0.9	685.6±1.0	1954.0±1.0	1.1	–1.9	30492

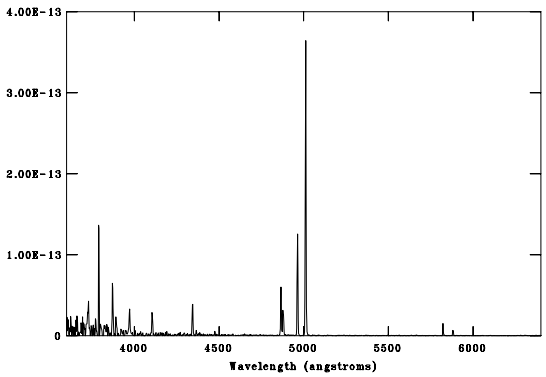

Fig. 1a. *Optical spectrum of SMP L8 coincident with J045013-693352.*

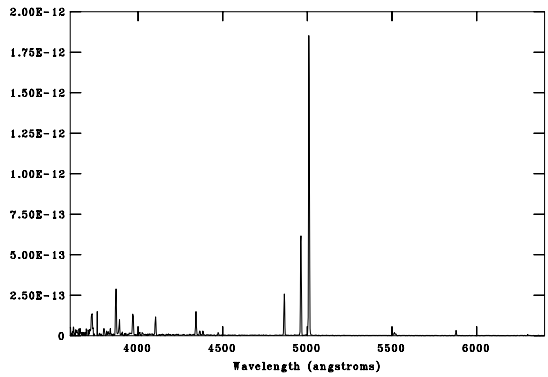

Fig. 1b. *Optical spectrum of SMP L25 coincident with J050624-690320.*

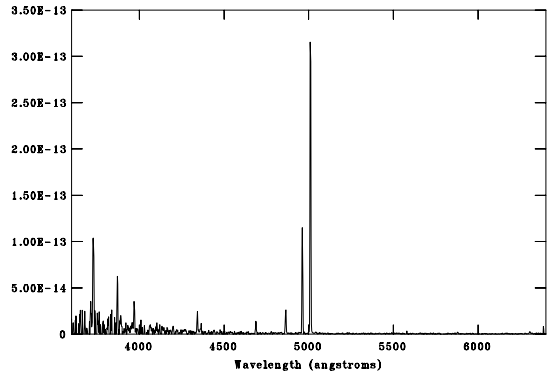

Fig. 1c. *Optical spectrum of SMP L33 coincident with J051009-682955.*

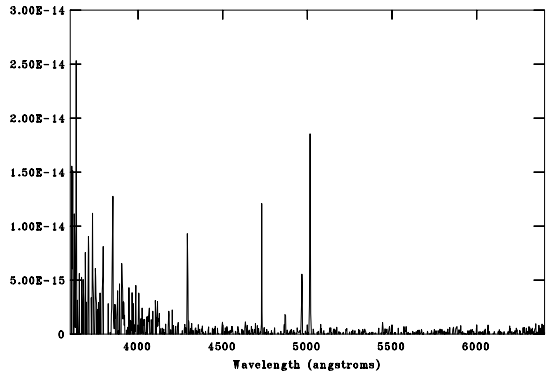

Fig. 1d. *Optical spectrum of SMP L39 coincident with J051142-683459.*

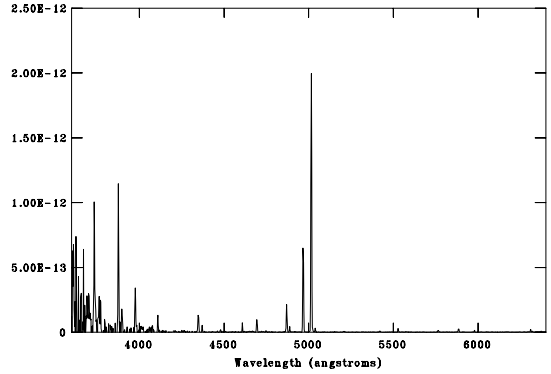

Fig. 1e. *Optical spectrum of SMP L47 coincident with J051954-693104.*

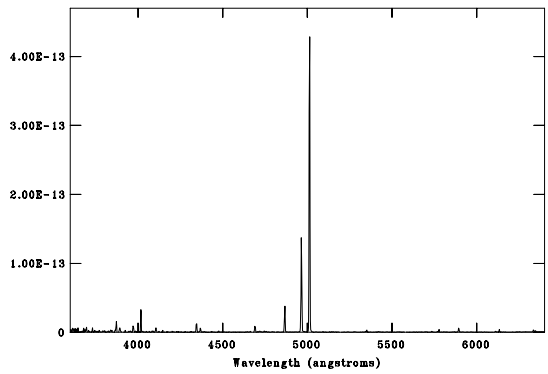

Fig. 1f. *Optical spectrum of SMP L62 coincident with J052455-713255.*

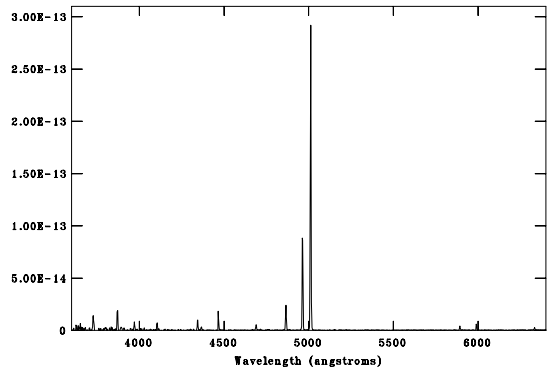

Fig. 1g. *Optical spectrum of SMP L74 coincident with J053329-715227.*

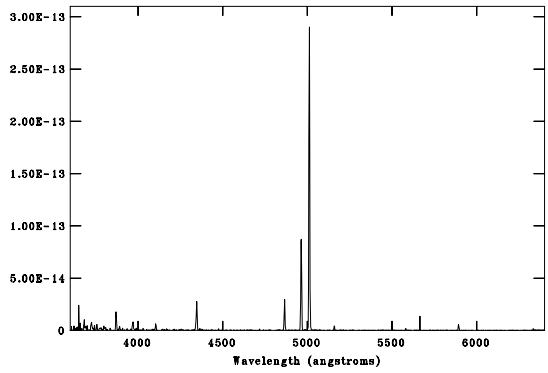

Fig. 1h. *Optical spectrum of SMP L75 coincident with J053346-683643.*

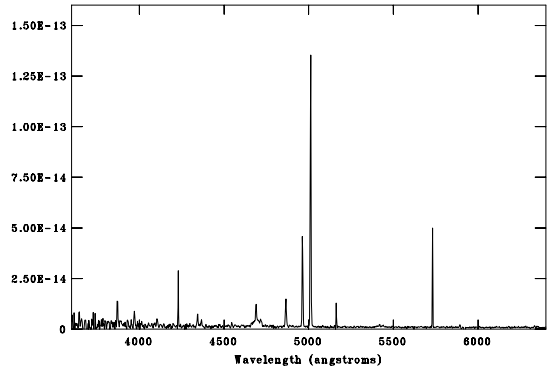

Fig. 1i. *Optical spectrum of SMP L83 coincident with J053620-671807.*

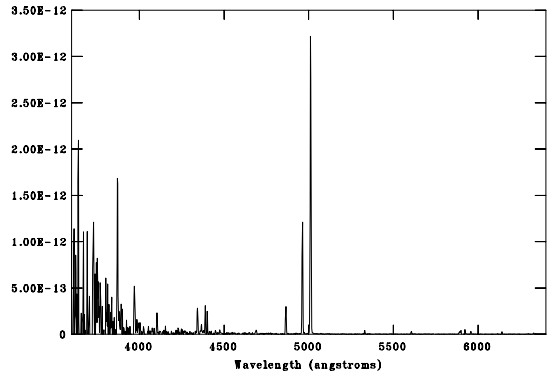

Fig. 1k. *Optical spectrum of SMP L89 coincident with J054237-700930.*

Extinction may be calculated using the Balmer emission lines: Hα6563Å, Hβ4861Å, Hγ4340Å and Hδ4102Å. Noting that our spectral range does not include Hα6563Å and that there is increased noise in many of the spectra near the Hδ4102Å line, we estimate Balmer decrements as Hγ/Hβ. Characteristic extinction curves are given by Osterbrock and Ferland (2006) and expected intrinsic Balmer decrements are based on Case B recombination[1]. Table 2 lists individual values for E(B–V) based on these decrements. We cannot accurately measure the Hγ4340Å line for SMP L39 and SMP L84 because of baseline noise (Fig. 1). Of the available decrements, the calculated extinctions are zero or less for all but one. Thus, three electron temperatures ($T_{\rm e}$) (SMP L39, SMP L62 and SMP L84) given in Table 2 may be affected, but their uncorrected values are reasonable, given the values are dependent on the [O III] forbidden line ratio having a maximum interval of 644Å.

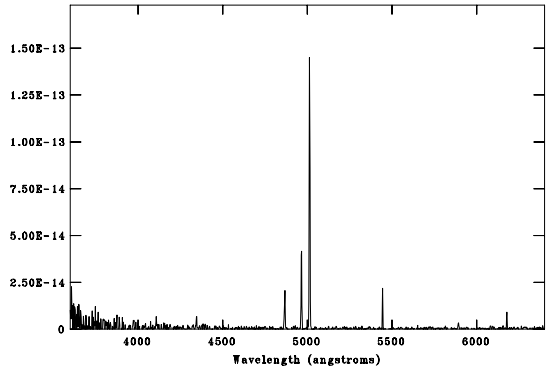

Fig. 1j. *Optical spectrum of SMP L84 coincident with J053653-715339.*

The 90% confidence errors reported in Table 2 are based on line measurement; we do not account for absolute photometric errors. Line measurement errors were calculated using Monte-Carlo simulation techniques found in the task SPLOT for a sample number of 100 and measured rms sensitivity. This 1σ value was multiplied by 1.64 to estimate a 90% confidence interval for each flux density.

Ions including [O III] and [N II] have energy-level structures that produce emission lines from different excitation energies. The relative rates of excitation depend very strongly on temperature and may be used to measure $T_{\rm e}$. The only practical probe for the measurement of electron temperature in our case is the [O III] forbidden line ratio[2]. We list electron temperatures in Table 2 for each of our nebulae, based on this [O III] ratio.

Since our spectral range excluded the [S II]6717, 6731Å lines needed to calculate electron densities, we assume a $n_{\rm e}$ of 10^3 cm^{-3} for this selected radio sample[3]. We base this approximate value on PNe averages found in Stanghellini and Kaler (1989) and estimate $T_{\rm e}$ using the Space Telescope Science Data Analysis System task NEBULAR.TEMDEN, based on a five-level atom approximation from De Robertis et al. (1987).

[1] An approximation characterized by large optical depth, where every Lyman-line photon is scattered many times and is eventually converted into lower-series photons.

[2] Defined as $\frac{\lambda 4959+\lambda 5007}{\lambda 4363}$.

[3] While the [O III] forbidden line ratio algorithm uses electron density, it should be noted that even a factor of 100 from the assumed 10^3 cm $^{-3}$ in electron density affects the calculated temperature by only a few hundred K at most.

Table 3. Ionized abundances for [O II], [O III] and [Ne III] given in N(X) / N(H^+) as determined by NEBULAR.IONIC.

Name	$O^+ \times 10^{-4}$ 3727Å Blend	$O^{+2} \times 10^{-4}$ 5007Å Line	$Ne^{+2} \times 10^{-5}$ 3869Å Line
SMP L8	—	0.08	0.36
SMP L25	0.06	0.65	2.50
SMP L33	0.86	1.90	8.13
SMP L39	—	—	—
SMP L47	0.46	0.58	7.27
SMP L62	0.04	1.40	1.63
SMP L74	0.15	1.79	3.58
SMP L75	—	1.96	3.66
SMP L83	—	0.39	0.87
SMP L84	—	—	—
SMP L89	—	0.28	3.65

Ion abundances are presented in Table 3, computed using NEBULAR.IONIC. This program determines ionic concentrations with respect to H^+ ions based on the flux (on a scale Hβ = 100) and the wavelength of a selected emission line. Comparison with values obtained for Galactic PNe, such as those presented by Bohigas (2001), suggest they are not unusual.

Table 4. Spectra containing prominent ionized [forbidden] iron emission lines (1 = flux much greater than Hβ; 2 = flux about equal to Hβ; 3 = flux much less than Hβ).

Name	Iron Emission Lines
SMP L39	[Fe II]4287Å(1)
SMP L83	[Fe V]4227Å(1)
	[Fe VII]5721Å(1)
SMP L84	[Fe VI]5427Å(2)

Figs. 1a through 1k show our one-dimensional spectra for each PNe listed in Table 2. These spectra have typical emission lines which we highlight here. In addition to the expected [O II], [O III] and Balmer lines, we note that several reveal a [Ne III]3869Å line (SMP L8, SMP L25, SMP L33, SMP L47, SMP L62, SMP L74, SMP L75, SMP L83 and SMP L89) common in PNe. Many also have a blend at 3968Å representing [Ne III]/Hϵ (SMP L25, SMP L33, SMP L47 and SMP L89). Other lines include He I3889, 4026, 4471, 5876Å and He II4686Å.

SMP L39, SMP L83 and SMP L84 show an assortment of ionized iron emission lines including [Fe II]4287Å, [Fe V]4227Å, [Fe VI]5427Å and [Fe VII]5721Å (see Table 4). In the previous paper (Payne et al. 2008), we also noted that JD10 in the SMC had a predominant [Fe III]4881Å line. This seemed unusual since the abundance of iron in PNe is scarcely studied, due to its relative faintness (Perinotto et al. 1999). Therefore, we are identifying a sub- population of PNe with prominent ionized iron lines that warrant further verification and study.

4. CONCLUDING REMARKS AND SUMMARY

Most observed PNe have nebular masses of only 0.3 $M_\odot$, although the main-sequence mass of PNe progenitors can be as high as 8 $M_\odot$ (Kwok 1994). The PNe studied here may represent a predicted "missing-mass link", belonging originally to a system possessing up to an 8 $M_\odot$ or higher central star. Given values of radio flux density at $\sim$ 5 GHz, we suggest that the ionized nebular mass of these PNe could be as high as 1.8 $M_\odot$ assuming an average density of 10^3 cm^{-3}.

High rates of mass loss that continue for an extended fraction of a AGB's lifetime can allow a significant fraction of the star's mass to be accumulated. This may result in the formation of a circumstellar envelope (CSE) or halo. If the transition from the AGB to PN stage is short, then such CSEs could have a significant effect. Perhaps our radio observations select for high mass PNe, since the quantity of ionized mass present is directly related to radio flux density.

Our combined observations suggest that a population of PNe in the MCs have bright radio counterparts, with nebular electron temperatures within a reasonable range given instrument resolution and sensitivity. Ionized abundances of [O II], [O III] and [Ne III] are not unusual. While most have typical spectra, at least a third have prominent forbidden ionized iron lines.

Acknowledgements – This paper uses observations made from the South African Astronomical Observatory (SAAO). Travel to the SAAO was funded by Australian Government, AINSTO AMRFP grant number 07/08-O-11. We thank the Serbian Ministry for Science for support (Projects 146012 and 146016). We also used the KARMA software package developed by the ATNF. The Australia Telescope Compact Array is part of the Australia Telescope which is funded by the Commonwealth of Australia for operation as a National Facility managed by CSIRO. IRAF is distributed by the National Optical Astronomy Observatories, which are operated by the Association of Universities for Research in Astronomy, Inc., under cooperative agreement with the National Science Foundation.

REFERENCES

Alves, D. R.: 2004, *New Astronomy Review*, **48**, 659.
Bohigas, J.: 2001, *Rev. Mex. Astron. Astrofis.*, **37**, 237.
De Robertis, M. M., Dufour, R., Hunt, R.: 1987, *J. Roy. Astron. Soc. Canada*, **81**, 195.
Dickel, J. R., McIntyre, J. J., Gruendl, R. A., Milne, D. K.: 2005, *Astron. J.*, **129**, 790.
Hughes, A., Staveley-Smith, L., Kim, S., Wolleben, M., Filipović, M. D.: 2007, *Mon. Not. R. Astron. Soc.*, **382**, 543.

Jacoby, G. H., De Marco, O.: 2002, *Astron. J.*, **123**, 269.
Kwok, S.: 1994, *Publ. Astron. Soc. Pacific*, **106**, 344.
Kwok, S.: 2000, "The Origin and Evolution of Planetary Nebulae", Cambridge University Press, Cambridge, p. 51.
Kwok, S.: 2005, *J. Kor. Astron. Soc.*, **38**, 271.
Osterbrock, D. E., Ferland, G. J.: 2006, "Astrophysics of Gaseous Nebulae and Active Galactic Nuclei (second edition)". University Science Books, Sausalito, p. 180.
Payne, J. L., Filipović, M. D., Crawford, E. J., de Horta, A. Y., White, G. L., Stootman, F. H.: 2008, *Serb. Astron. J.*, **176**, 65.
Payne, J. L., Filipović, M. D., Reid, W., Jones, P. A., Staveley-Smith, L, White, G. L.: 2004, *Mon. Not. R. Astron. Soc.*, **355**, 44.
Perinotto, M., Bencini, C. G., Pasquali, A., Manchado, Rodriguez Espinosa, J. M., Stanga, R.: 1999, *Astron. Astrophys.*, **347**, 967.
Reid, W. A., Parker, Q. A.: 2006, *Mon. Not. R. Astron. Soc.*, **373**, 521.
Sanduleak, N., MacConnell, D. J., Philip, A. G. Davis: 1978, *Publ. Astron. Soc. Pacific*, **90**, 621.
Stanghellini, L., Kaler, J. B.: 1989, *Astrophys. J.*, **343**, 811.

ОПТИЧКИ СПЕКТРИ РАДИО ПЛАНЕТАРНИХ МАГЛИНА У ВЕЛИКОМ МАГЕЛАНОВОМ ОБЛАКУ

J. L. Payne[1], M. D. Filipović[2], W. C. Millar[1], E. J. Crawford[2], A. Y. De Horta[2], F. H. Stootman[2] and D. Urošević[3]

[1] *Centre for Astronomy, James Cook University*
Townsville QLD, 4811, Australia

E–mail: *snova4@msn.com*

[2] *University of Western Sydney, Locked Bag 1797,*
Penrith South DC, NSW 1797, Australia

[3] *Department of Astronomy, Faculty of Mathematics, University of Belgrade*
Studentski trg 16, 11000 Belgrade, Serbia

УДК 524.37-355.3 : 524.722.3
Оригинални научни рад

У овој студији представљамо прелиминарне резултате спектралне анализе 11 (од познатих 12) радио кандидата за планетарну маглину у Великом Магелановом Облаку (ВМО). Оптичка посматрања приказана овде урађена су са Радклиф 1.9-m телескопом (Садерленд, Јужна Африка). Ових 11 радио планетарних маглина оригинално су откривене у нашим ранијим радио-прегледима ВМО направљеним Аустралијским Телескопом Компактног Поља (ATCA) на 20, 6 и 3 cm, а такође су потврђене додатним посматрањима високе резолуције на 6 и 3 cm ($4''/2''$). Оптичке и радио-позиције ових 11 кандидата за радио планетарне маглине у ВМО су удаљене мање од $2''$ и највероватније представљају подпопулацију планетарних маглина изражених као веома сјајни радио-објекти. Јонизоване масе ових маглина су прорачунате на до 1.8 $M_\odot$, што даље подржава постојање планетарних маглина са масивним (до 8 $M_\odot$) прогениторским централним звездама које губе већи део своје масе у АГБ фази или чак пре ове фазе. Такође смо идентификовали и подпопулацију (33%) радио планетарних маглина са проминантним емисионим линијама гвожђа.